Novel surface electrode design for preferential activation of cutaneous nociceptors

Poulsen, Aida Hejlskov; van den Berg, Boudewijn; Arguissain, Federico G; Tigerholm, Jenny; Buitenweg, Jan R; Andersen, Ole Kaeseler; Mørch, Carsten Dahl

Published in:
Journal of Neural Engineering

DOI (link to publication from Publisher):
10.1088/1741-2552/ac4950

Publication date:
2022

Document Version
Accepted author manuscript, peer reviewed version

Journal of Neural Engineering

Novel surface electrode design for preferential activation of cutaneous nociceptors

To cite this article before publication: Aida Hejlskov Poulsen *et al* 2022 *J. Neural Eng.* in press https://doi.org/10.1088/1741-2552/ac4950

Novel surface electrode design for preferential activation of cutaneous nociceptors

Aida Hejlskov Poulsen[1], Boudewijn van den Berg[2], Federico Arguissain[1], Jenny Tigerholm[1], Jan R. Buitenweg[2], Ole Kæseler Andersen[1], Carsten Dahl Mørch[1]

[1] Center for Neuroplasticity and Pain (CNAP), Department of Health Science and Technology, Aalborg University, Aalborg, Denmark

[2] Biomedical Signals and Systems, Technical Medical Centre, University of Twente, PO Box 217, 7500 AE Enschede, The Netherlands

Abstract

Objective Small area electrodes enable preferential activation of nociceptive fibers. It is debated, however, whether co-activation of large fibers still occurs for the existing electrode designs. Moreover, existing electrodes are limited to low stimulation intensities, for which behavioral and physiological responses may be considered less reliable. A recent optimization study showed that there is a potential for improving electrode performance and increase the range of possible stimulation intensities. Based on those results, the present study introduces and tests a novel planar concentric array electrode design for small fiber activation in healthy volunteers.

Approach Volunteers received electrical stimulation with the planar concentric array electrode and a regular patch electrode. Perception thresholds were estimated at the beginning and the end of the experiment. Evoked cortical potentials were recorded in blocks of 30 stimuli. For the patch, stimulation current intensity was set to two times perception threshold (PT), while three intensities, 2, 5, and 10 times PT, were applied with the planar concentric array electrode. Sensation quality, numerical-rating scores, and reaction times were obtained for each PT estimation and during each block of evoked potential recordings.

Main results Stimulation with the patch electrode was characterized as dull, while stimulation with the planar concentric array electrode was characterized as sharp, with increased sharpness for increasing stimulus current intensity. Likewise, scores of the numerical rating scale were higher for the planar concentric array electrode compared to the patch and increased with increasing stimulation current intensity. Reaction times and ERP latencies were longer for the planar concentric array electrode compared to the patch.

Significance The presented novel planar concentric array electrode is a small, non-invasive, and single-use electrode that has the potential to investigate small fiber neuropathy and pain mechanisms, as it is small fiber preferential for a wide range of stimulation intensities.

1. Introduction

Selective activation of specific nerve fiber populations has enormous value in understanding the functioning of different subsystems of the human nervous system. Among other applications, selective activation can help identify functions of different fiber types and to diagnose and follow treatment outcomes in pathologies of peripheral nerve fibers. Because of the great potential in pain conditions, selective activation of cutaneous nociceptors has been a hot topic for the last 40 years. However, most of the methods used in research display technical limitations that have prevented their clinical use and availability [1]. Addressing these issues may facilitate the implementation of research methods in clinical applications.

For nociceptive activation, laser stimuli are often used and evaluated by analyzing the evoked potentials (EP) and the behavioral responses to the stimuli [2]. Nonetheless, laser stimulation has certain technical constraints that currently limit its use. Laser stimulation poses a high risk of skin lesions and requires extended safety precautions and expert personnel to manipulate it [2]–[5]. Furthermore, laser stimulation require time for heat conduction and transduction of the heat into a neuronal signal. Electrical, on the other hand, stimulation bypasses receptors and activate the nerve directly, making the activated afferent volley more synchronous compared to laser activation.

Thus, electrical stimulation poses a safe, easy to control, and cheap alternative to laser and is already extensively used in the clinical assessment of large non-nociceptive nerve fiber afferents. Yet, conventional electrical stimulation suffers from a lack of specificity since the activation threshold of nociceptors is higher than the threshold of non-nociceptive fibers. Consequently, a high-intensity stimulus will co-activate a significant amount of tactile nerve fibers, contaminating the nociceptive input. Several specialized electrodes have been designed to overcome this limitation [6]–[9]. Common for these electrodes is the small cathode area, which enables the generation of a high current density in the proximity of nociceptive nerve fiber endings and thereby achieves preferential activation of nociceptors [9]–[11]. These specialized electrodes have recently displayed the potential to assess small fiber function and follow patient outcomes in certain neuropathic conditions. Both perception thresholds (PT) and features of pain-related EPs elicited by these specialized electrodes correlated with disease duration and progression in patients with HIV- and diabetes-related neuropathies [12]–[14].

Despite these promising results, the small fiber selectivity of these electrodes has been highly debated, and results of EP latencies studies of healthy volunteers have indicated preferential Aδ-fiber activation [15], [16] as well as substantial co-activation of Aβ-fiber [17], [18].. Differences between studies likely arise due to differences in stimulation current intensity. When increasing the stimulation current intensity, the current may reach deeper tissues and cause co-activation of large non-nociceptive fibers. Therefore, low stimulation intensities around two times PT have been recommended [3], [19]. Nonetheless, this recommendation may only be relevant to one specific electrode design since current density is dependent on the electrode shape and type [11]. Moreover, all of the existing electrodes have been developed empirically and may be further optimized to increase nociceptive specificity and the applicable range of stimulation intensities [20]. Poulsen *et al.* (2021) showed that minimizing the electrode dimensions would increase preferential activation of

small fibers. The present study aimed to provide a first exploration of a novel planar concentric array electrode design following the recommendations of electrode dimensions from the purely computational study of Poulsen *et al.* (2021).

2. Methods

2.1 Subjects

A total of 25 healthy volunteers (14 females and 11 males), aged 26-57 (average 32), participated in the experiment. Subjects were novices and had no previous knowledge about the study objective. Written informed consent according to the Declaration of Helsinki was obtained from all participants. The experimental study was approved by the local ethics committee (ref. no N-20180050).

2.2 Stimulation electrodes

Evoked potentials were elicited by two different electrodes: a regular patch electrode (3 cm^2, Ambu® neuroline 700) with a large area anode (75 cm^2, DJO™ brands, Dura-stick premium 42207) and a newly developed planar concentric array electrode for preferential small fiber activation (see figure 1). The cathode of the regular patch electrode setup was placed on the volar forearm 5 cm distal to the elbow joint, while the anode was positioned at the wrist. The planar concentric array electrode consisted of seven interconnected concentric silver electrodes printed on a flexible PET base (Screentec, Oulu, Finland). An additional layer of thin carbon was printed onto the cathodes. The cathodes had a diameter of 0.5 mm. The anodes were concentric circles with an inner diameter of 1.5 mm and an outer diameter of 2.1 mm. The planar concentric array electrode was positioned on the volar forearm with the center of the electrode 5 cm distal to the elbow joint, contralateral with respect to the regular patch electrode.

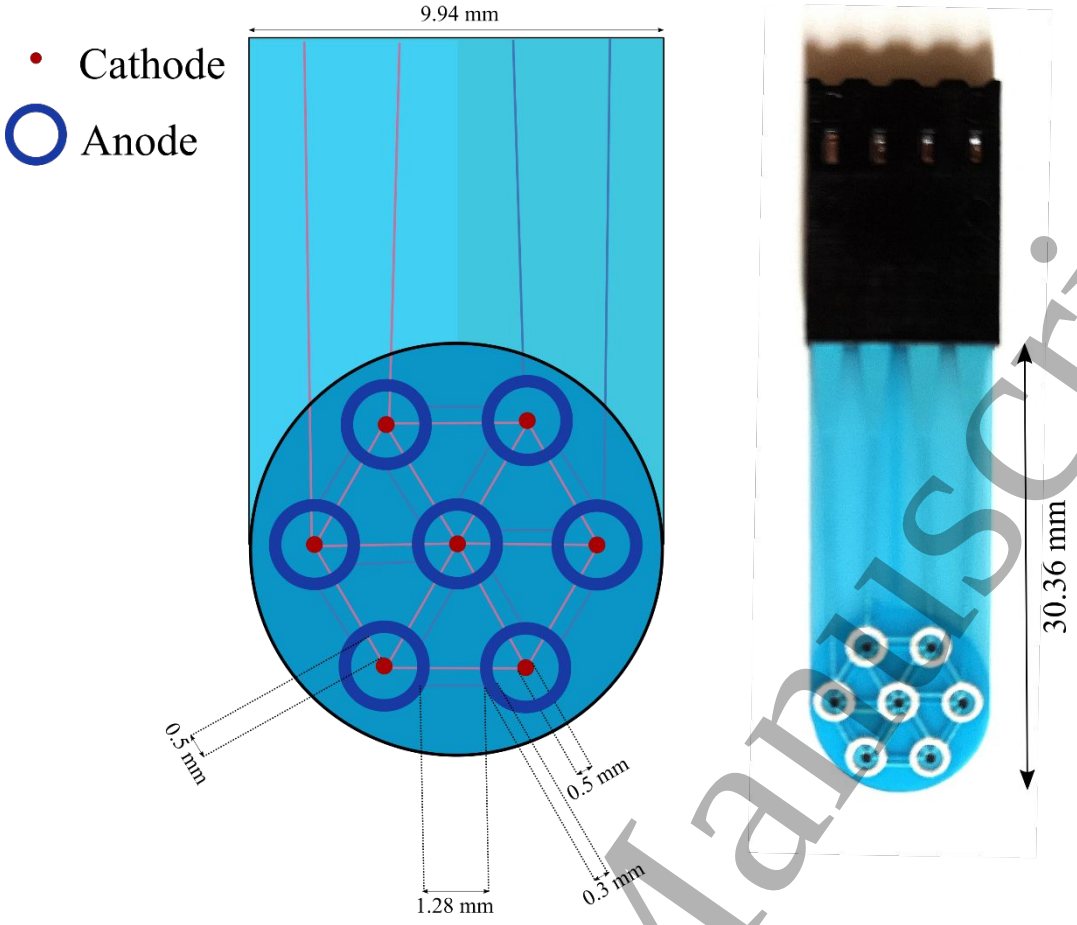

Figure 1 : Schematic representation and picture of the small fiber preferential electrode (not drawn to scale). The electrode consisted of 7 interconnected cathodes and 7 interconnected anodes in a cathode-anode pair setup. Cathodes represented in red had a diameter of 0.5 mm. The anodes presented in blue were concentric circles around the cathodes and had a width of 0.3 mm. The anode-cathode distance was 0.5 mm, and the distance between the outer borders of the anodes was 1.28 mm. The electrode pairs were printed on a flexible PET base with a width of 9.94 mm and a length of 30.36 mm.

2.3 Experimental procedure

The overall experimental procedure is illustrated in figure 2. The prepping procedure included the setup and connection of the EEG equipment and preparation of the skin. Hairs were removed by shaving, and subsequently, the skin was gently rubbed and cleaned with alcohol. Electrical stimulation was delivered with a constant current stimulator (DS5; Digitimer, Ltd., UK), controlled by a custom-made program (LabBench; Aalborg University, Denmark). Prior to estimating the perception threshold (PT), the subject was familiarized with the stimulus sensation and the PT estimation procedure through a small training session. The PT was determined at the beginning and end of the experiment. EEG was recorded in blocks of 30 stimuli (EEG blocks). For the planar concentric array electrode, a total of 3 blocks of 30 stimuli were applied, with fixed intensities of 2, 5, and 10 times the initial PT. A five-minute break separated the blocks. Only one block of 30 stimuli was applied for the patch electrode at a stimulation current intensity of 2 times PT. The stimulation

side (left or right arm) and order of the electrodes were randomized between subjects. A single stimulus consisted of a train of three charge-balanced pulses of 0.5 ms duration with an inter-pulse-interval of 10 ms. Thereby each block of stimulation included 30 pulse trains. The interval between pulse trains was randomized between 8-15 seconds in an attempt to minimize habituation effects. The subject was asked to rate the perception of the stimulation on a numerical rating scale (NRS) and a description scale ranging from dull to sharp after each determination of PT and after each EEG stimulation block.

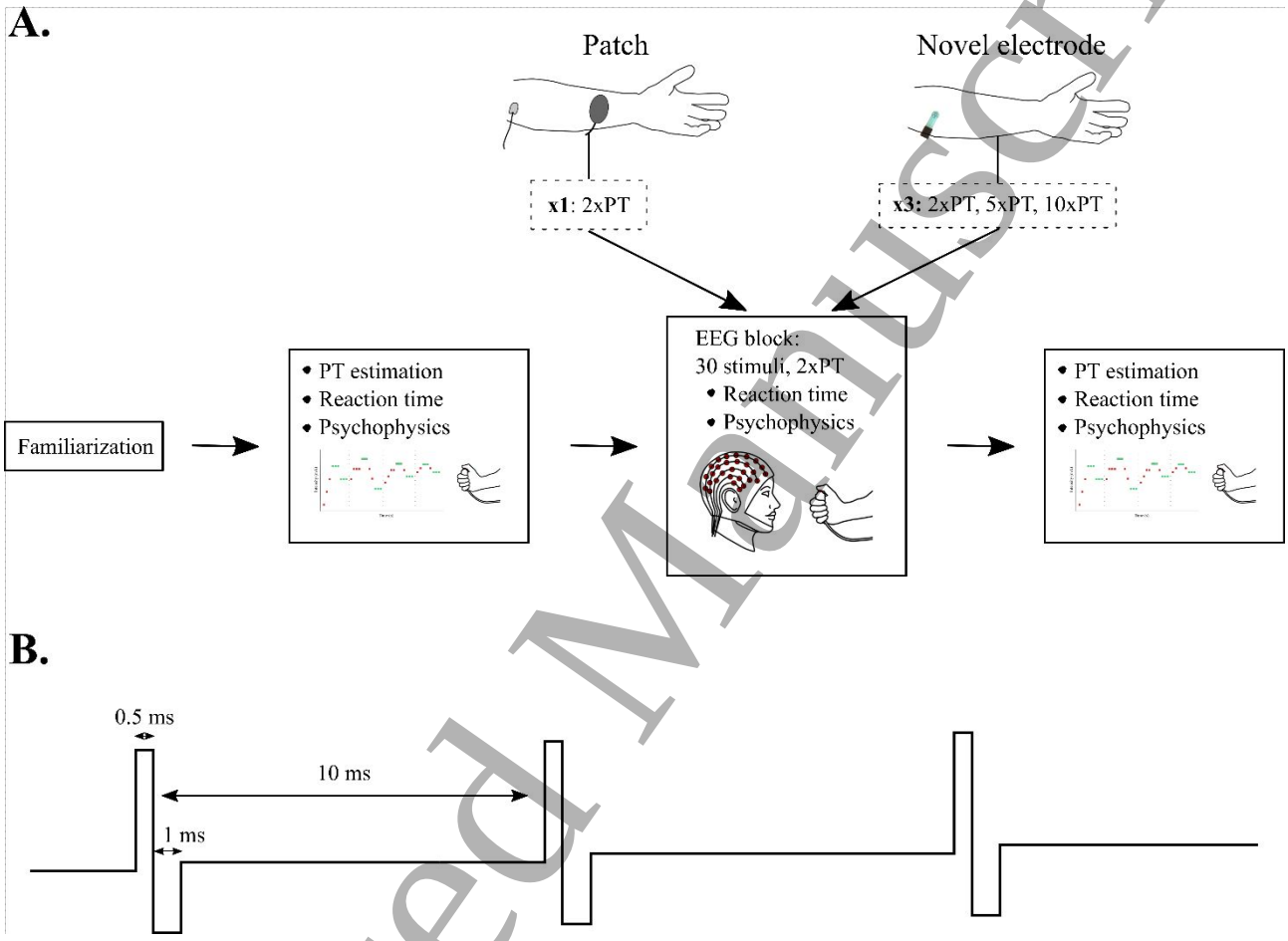

Figure 2: Overview of the experimental procedure. A. Initially, the site of electrode attachment was prepped. Subsequently, the subject was familiarized with the electrode sensation and perception threshold (PT) determination procedure in a short training sequence. PT was estimated at the beginning and the end of the experiment. 3 non-randomized sequential EEG blocks were conducted for the planar concentric array electrode (stimulus current intensity of 2,5 and 10xPT), while 1 EEG block was conducted for the patch electrode (stimulus current intensity of 2xPT). The order of the electrodes was randomized between subjects (13 subjects started with the planar concentric array electrode, and 12 subjects started with the patch electrode). The subject had a five-minute break between EEG blocks. Reaction times were recorded simultaneously with the electrical stimulation, both during the PT estimation and the EEG blocks. Psychophysical measures about the stimulus sensation were obtained after each stimulation (PT estimation and EEG Blocks). B. Stimulus pulse design. A train of three charge-balanced rectangular pules was used as stimulus.

2.4 Perception threshold estimation

Initially, a short PT determination with two ascending and two descending limits were performed in order to familiarize the subject to the procedure of PT determination and to familiarize the subject with the nature of the electrical stimulation and the sensations elicited by the electrodes. This gave the subject an opportunity to get comfortable with the stimulation and the experiment. Psychophysical data was not recorded for the familiarization and the estimated PT was discarded. Subsequent to the familiarization the PT was determined by a modified method of limits [11], [21], with four ascending and descending limits. The limits were defined as three consecutive perceived or unperceived stimuli at the same current intensity. The stimulation current intensity increased or decreased by 20 %, 12 %, 8%, and 5% for each pair of ascending and descending limits. The starting value for the stimulus current intensity was 0.1 mA, and the subjects were instructed to push a button as fast as possible whenever a stimulus was perceived. The final threshold was defined as the weighted average of the eight limits (4 ascending and 4 descending), with weights corresponding to the inverse of the step size.

2.5 Psychophysics

After each PT estimation and each block of EPs recordings, the subject was asked to rate the sensation on a visual analog scale (VAS) from dull to sharp (n=14) or from sharp to dull (n=11), and on an NRS scale ranging from “no sensation” (0) to “worst imaginable pain” (100), with 30 representing the pain threshold.

2.6 Reaction Times

Reaction times were recorded during both the PT estimation and the EEG blocks. The subject was instructed to push a button as fast as possible whenever a stimulus was perceived. For the PT estimation, only reaction times at the ascending limits were used for further analysis (12 reaction times in total). Reaction times below 100 ms (0.11 % of all trials) or above 1000 ms (0.19 % of all trials) were considered to be results of anticipation, fast guessing, or poor attention and were thus defined as undetected stimuli.

2.7 Electrophysiological measures

EPs were recorded for each block of 30 stimuli using a g.HIamp amplifier, g.scarabeo (Ag/AgCl) active electrodes, and the g.Recorder software by g.tec medical engineering GmbH, Austria. A total of 32 channels were recorded according to the international 10-20 system. in. An electrode placed at the left earlobe served as reference. The signal was sampled at 2000 Hz, and electrode impedances were kept below 10 kΩ. Subjects were instructed to blink as little as possible during the stimulation block. EEG preprocessing was performed using the MATLAB (The Mathworks Inc, USA) toolboxes EEGLAB [22] and Letswave 6 (Université Catholique de Louvain, Belgium). In EEGLAB, the continuous EEG data was band-pass filtered from (0.5-40 Hz) and subsequently downsampled (250 Hz). Bad channels were interpolated, and the data were segmented into epochs ranging from -0.5 s to 1.0 s relative to stimulus onset. All epochs were baseline corrected by subtracting the average signal prior to stimulus onset (-0.5 s to 0 s). Channels were considered bad; if they contained flatline periods

of more than 5 seconds, if the line noise relative to the channel signal exceeded 5 times the standard deviation, or if the channel correlation with nearby channels were less than 0.85. The identified bad channels were interpolated with the spherical method implemented in the EEGLAB. Letswave was used to perform an independent component analysis to identify and remove eye blinks and movement artifacts. Components with distinct wave patterns and scalp distributions indicating the equivalent dipole to be close to the eyes were removed. Furthermore, high frequency activity resembling muscle activity and with clear scalp distributions close to the jaw muscles were removed.. For stimuli applied to the left arm, the EEG channels were flipped over the midline.

2.8 Statistical analysis

Linear mixed modeling was used to investigate differences between electrodes and intensities for the PT, psychophysics, reaction times, and EP waves. The PT, psychophysics, and reaction times were log-transformed prior to analysis, as they were not normally distributed. The equations of the linear mixed models are presented in Wilkinson notation [23], in which the random effect term is written inside brackets, and the '|S' denotes grouping of the random effects term by subject.

PTs were compared between electrodes. The model included fixed effects of the electrode, test (initial and final PT determination), and the interaction between electrode and test. A maximal random effects term was used to account for between-subject variability (see equation 1).

$$PT \sim 1 + Elec + Test + Elec * Test + (1 + Elec + Test + Elec * Test \,|\, S)\ \#(1)$$

For the psychophysical measures of NRS scores and the dull-sharp VAS descriptor, two models were constructed, one for the comparison of electrodes and one for the comparison of intensities applied with the planar concentric array electrode (see equation 2 and 3). The model for the psychophysics electrode comparison included fixed effects of the electrode, current intensity (PT and 2xPT), and electrode-intensity interaction. The model for the psychophysics intensity comparison included the intensity as a fixed effect. For both models of the psychophysical data, a maximal random effects term was used to account for between-subject variability.

$$PSY_{elec} \sim 1 + Elec + Int + Elec * Int + (1 + Elec + Int + Elec * Int \,|\, S)\#(2)$$

$$PSY_{int} \sim 1 + Int + (1 + Int \,|\, S)\ \#(3)$$

Where PSY_{elec} denotes the electrode comparison, PSY_{int} denotes the intensity comparison.

Similar to the psychophysics analysis, two models were constructed for the reaction times, one for comparing electrodes and one for the comparison of intensities applied with the planar concentric array electrode (see equations 4 and 5). The model of the comparison of electrode reaction times included fixed effects of the electrode, current intensity (PT and 2xPT), and trial number. The model for comparison of intensity reaction times included fixed effects of intensity and trial number. For both models of reaction times, a maximal random effects term was used to account for between-subject variability.

$$RT_{elec} \sim 1 + Elec + Int + Trial + (1 + Elec + Int + Trial \,|\, S)\ \#(4)$$

$$RT_{int} \sim 1 + Int + Trial + (1 + Int + Trial \,|\, S)\ \#(5)$$

Data are reported as mean values and 95% confidence intervals.

2.8.1 Grand evoked potential prediction and evoked potential statistics

Eps were analyzed using a single-trial approach based on linear mixed regression [24], [25]. Similar to other multivariate single-trial approaches [26], a regression model is used to estimate the contribution of trial parameters (i.e., electrode type, stimulation current intensity, trial number) to the EEG at each sample. Between-subject variability was accounted for by using a maximal random effects term [27]. A model for the electrodes and a model for the stimulation current intensity level of the planar concentric array electrode were applied separately, as two additional current intensity levels were assessed for the planar concentric array electrode. The model of the electrodes included fixed effects of the electrode, trial number, and the order of the electrodes (see equation 6). Similarly, the model of the stimulus current intensity included the current intensity and the trial number as the fixed effect (see equation 7).

$$U_{EEG} \sim 1 + Elec + Trial + EOrder + (1 + Elec + Trial + EOrder \,|\, S) \quad \#(6)$$

$$U_{EEG} \sim 1 + Int + Trial + (1 + Int + Trial \,|\, S) \quad \#(7)$$

Subsequently, the models were used to predict the EP waveform (grand evoked potential prediction, GEPP) for each electrode and stimulation current intensity (see figure 3). Note that the GEPP is analogous to the grand average EP while accounting for potential confounding of habituation (i.e., the effect of trial number) and using the full set of trials to attenuate noise [24]. At the N1, N2, and P2 component latencies, the significance of electrode and stimulus current intensity effects were assessed using t-statistics. The N1, N2, and P2 components of the EP were identified and defined in terms of wave succession and scalp topographies [17], [28]. N1 was defined as the earliest negative component, within 80-170 ms after stimulus onset and with maximum amplitude at the contralateral temporal electrodes. The N1 peak was identified using the T7-Fz lead, as it is best observed on a bipolar configuration between the contralateral temporal and frontal electrodes [28]–[30]. N2 was defined as the first negative peak recorded at Cz, within 120-230 ms after stimulus onset. P2 was defined as the positive component at Cz, immediately following the N2 component, with latencies between 250 and 400 ms after stimulus onset and a midline predominance.

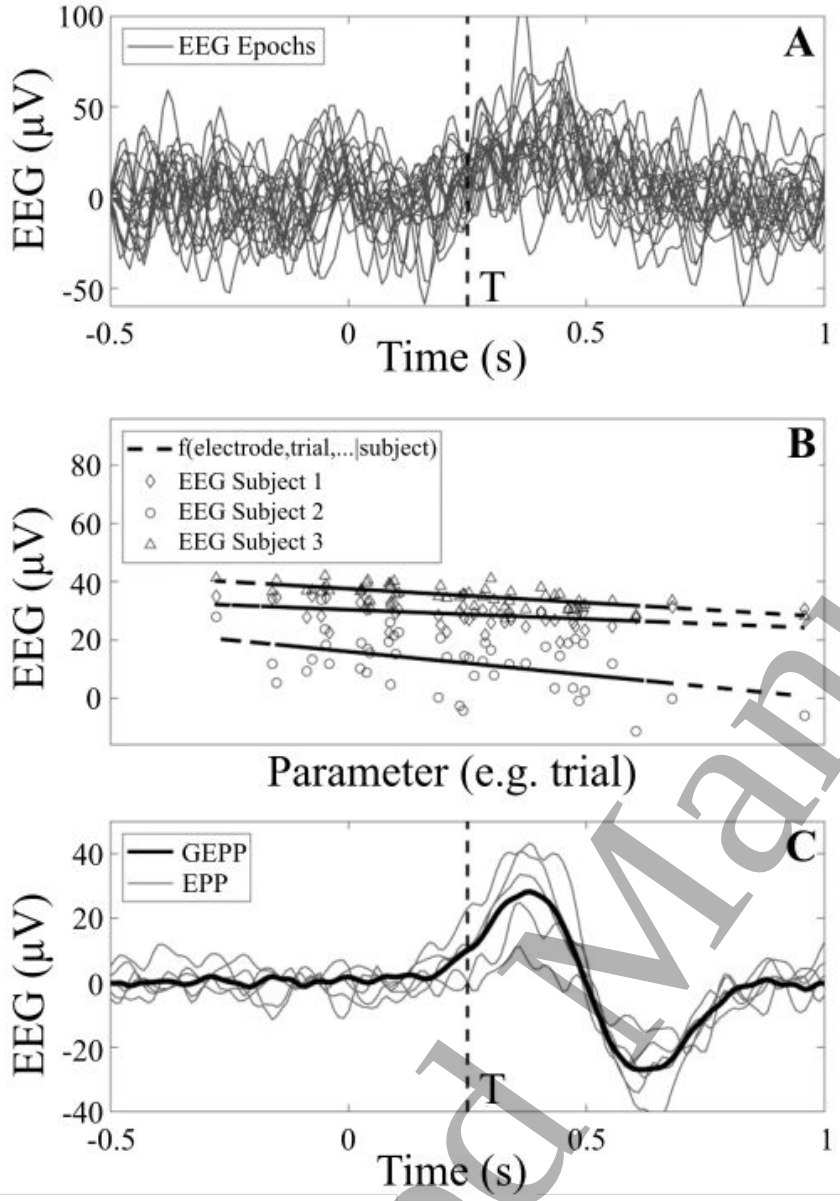

Figure 3: The linear mixed regression approach used to estimate and statistically test evoked potential waveforms. The EEG at each latency T, corresponding to each sample in the data, (A) is used to fit a multivariate mixed regression model (B). The linear mixed regression model is used to estimate the evoked potential waveform at time T for each subject (evoked potential prediction, EPP) or all subjects (grand evoked potential prediction, GEPP) (C). Adapted from van den Berg et al. (2020) [25].

3. Results

The PT of the planar concentric array electrode was significantly lower than the PT for the patch electrode (see figure 4, $p<0.01$). Furthermore, significant differences between the initial and final PT estimation ($p<0.01$) and significant interaction between electrode and PT test were observed ($p<0.01$). Analysis of the interaction showed significant increase of both the planar concentric array electrode PT (0.236 mA (95% Cl: 0.193-0.288) vs. 0.416 mA (95% Cl: 0.339-0.512)) and for the patch

electrode (0.582 mA (95% Cl: 0.477-0.710) vs. 0.636 mA (95% Cl: 0.525-0.772)). However, the increase in PT was larger for the planar concentric array electrode.

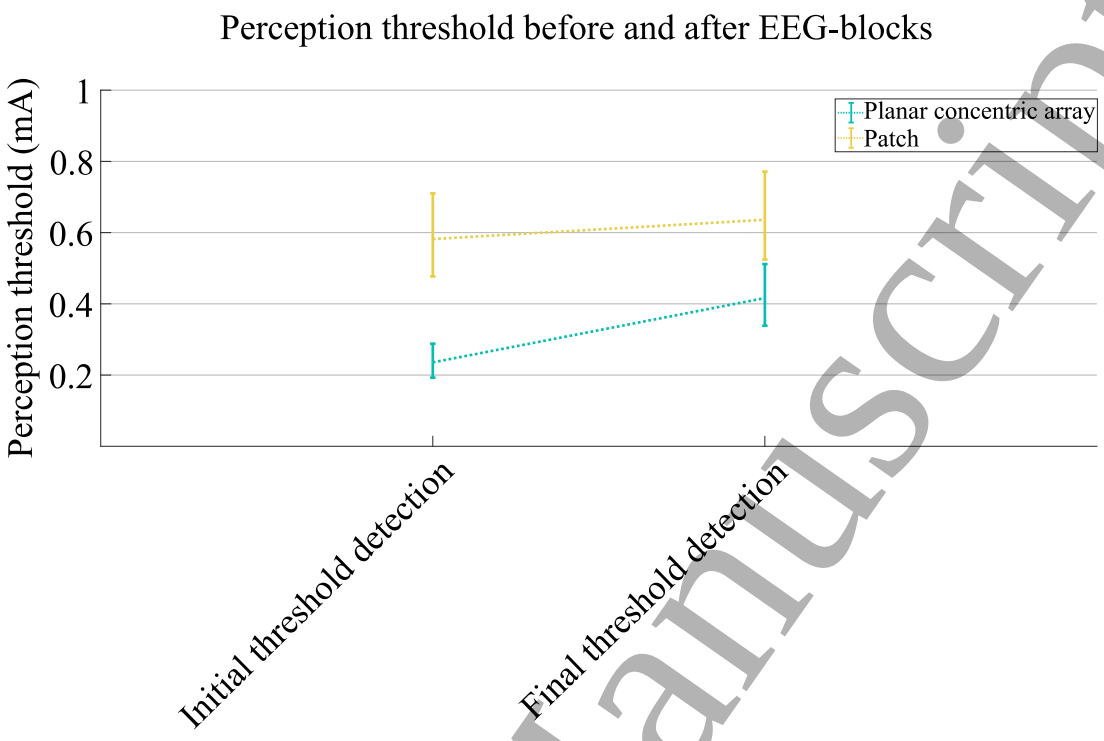

Figure 4: Average and 95 % confidence intervals of the perception thresholds at the initial threshold detection and the final detection, prior and subsequent to the EEG-blocks.

Average NRS scores and 95 % confidence interval for the patch and planar concentric array electrode at different intensities are presented in figure 5. The NRS scores were lower for the patch electrode 8.16 (95% Cl: 5.60-11.87) compared to the planar concentric array electrode 12.89 (95% Cl: 8.54-19.44) ($p<0.001$). For the patch electrode, the sensation was rated higher for stimuli at 2xPT compared to stimulations around the PT ($p<0.001$). A similar relation between intensities was not observed for the planar concentric array electrode. The planar concentric array electrode was rated as sharper than the patch electrode (see figure 6), with a significant effect of current intensity and electrode- current intensity interaction ($p<0.005$).

NRS scores for stimulation with the planar concentric array electrode increased with increasing current intensity. Significant differences were observed for all other intensities than the PT and 2xPT ($p<0.001$). The same pattern was displayed for stimulus sensation with no difference between the PT and 2xPT level but otherwise increased sharpness for increased current intensity.

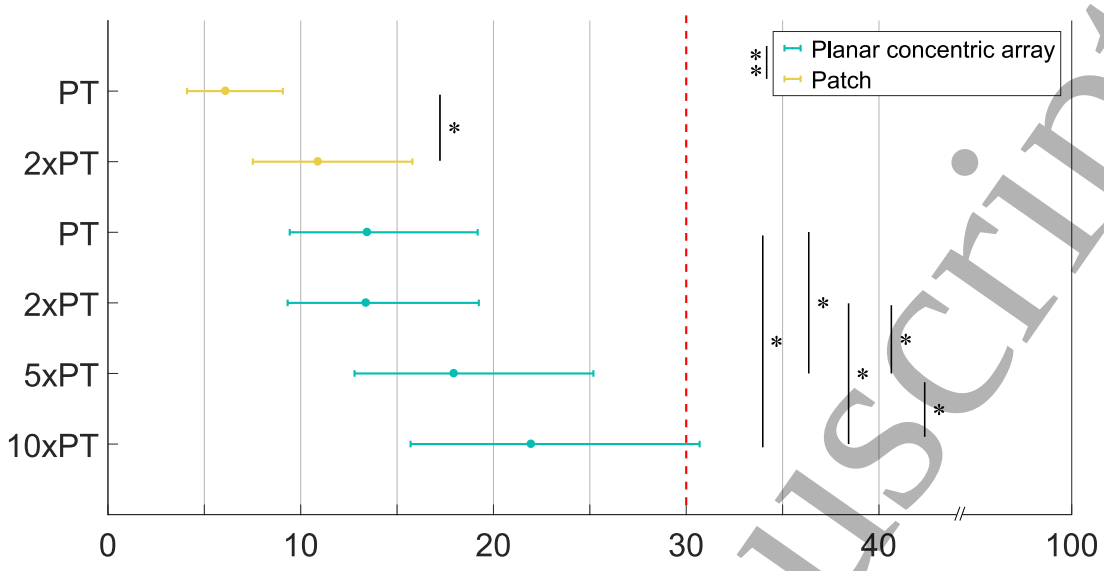

*Figure 5: Average and 95% confidence interval of the NRS scores on a scale from 0 to 100, with 30 marking the pain threshold. Data is presented by the log-transformed NRS scores as used in the statistical analysis. Significant differences were detected between electrodes (indicated by **, $p<0.005$) and between intensities for the planar concentric array electrode (indicated by *, $p<0.001$). For the intensities 5 and 10xPT displayed higher ratings than did stimulation at PT level and at 2xPT. Furthermore, 10xPT had higher NRS scores than 5xPT.*

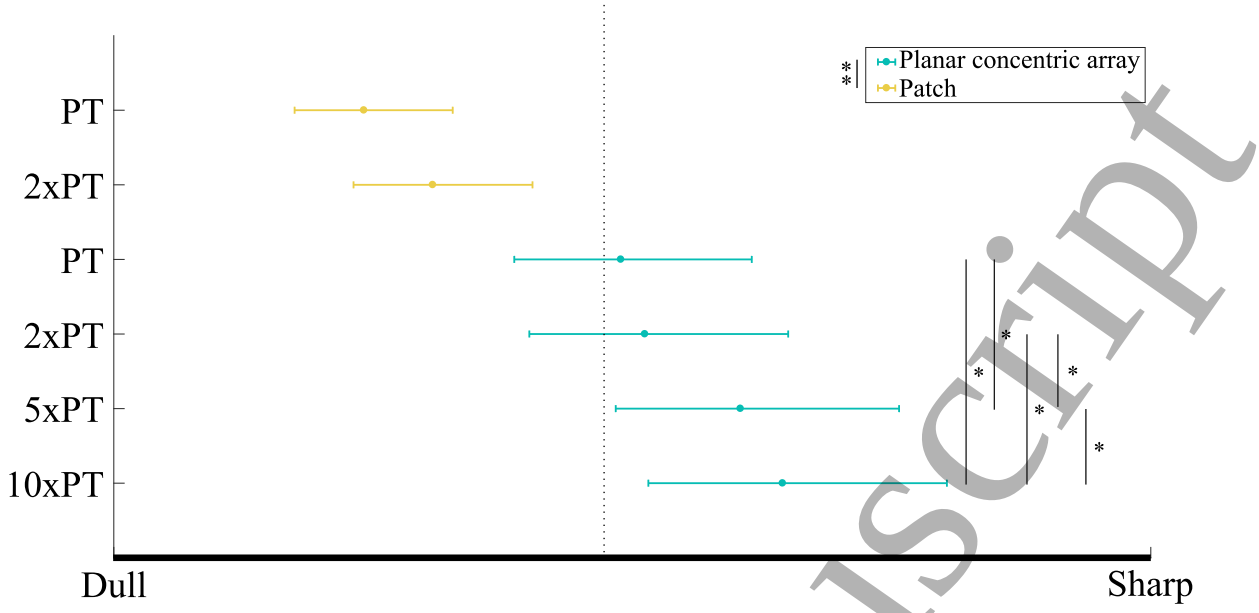

*Figure 6: Average and 95% confidence interval of the VAS scale for the descriptor of perceived stimuli from dull to sharp. To the right of the dashed line the stimuli was considered more dull than sharp, while ratings to the right of the line was considered sharp rather than dull. Significant differences were detected between electrodes (indicated by **, p<0.001). For the intensity comparison of the planar concentric array electrodes, 5 and 10xPT were rated to be sharper than 2xPT and the PT level. Additionally, 10 times perception was rated sharper than 5xPT (indicated by *, p<0.05).*

Reaction times were significantly longer for the planar concentric array electrode compared to the patch ($p<0.05$, see figure 7A). The reaction times were 373 ms (95% Cl: 342-408) for the planar concentric array electrode and 347 ms (95% Cl: 318-379) for the patch. Additionally, a significant effect was observed for the stimulus current intensity, with shorter reaction times at 2xPT than at PT. However, the interaction of electrode and current intensity revealed that the main effect of current intensity was mainly due to changes in the reaction times for the patch electrode. Furthermore, there was a significant effect of current intensities for the planar concentric array electrode with 5xPT and 10x PT displaying shorter reaction times than PT and 2xPT (see figure 7B).

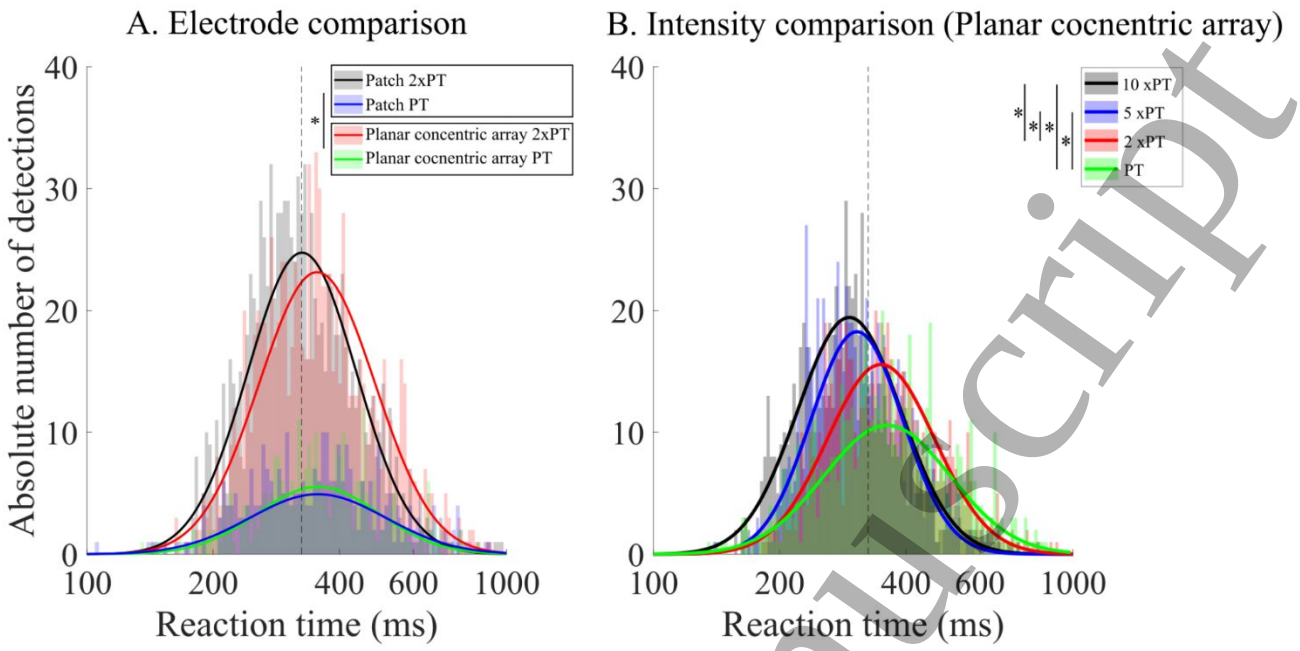

*Figure 7: Histogram of the log-transformed reaction times. (A) Electrode comparison, including reaction times for stimulations at PT and 2xPT. (B) Comparison of stimulation intensity with the planar concentric array electrode. * Indicates significant differences ($p<0.05$). The dashed line represents the expected limit between reaction times elicited by Aβ-fiber activity and Aδ-fiber activity* [31]. *Aβ-fibers were expected to lie to the left of the line, while Aδ-fibers were expected to lie to the right of the line.*

The GEPPs for the patch and planar electrode are presented in figure 8, and the corresponding latencies and amplitudes of the linear mixed model predicted N1, N2, and P2, are detailed in table 1. The predicted latencies of the EP waves were 12-20 ms longer for the planar concentric array compared to the patch. For the different intensities of the planar concentric array electrode, the N2 amplitude increased as the intensity increased. Additionally, the latency of the EP waves decreased with increasing intensity, most pronounced for the P2 component. The scalp topographies at the predicted N1, N2, and P2 latencies are illustrated in figure 9. For the N1 component, the patch topography had a lateral distribution restricted to the temporal electrodes contralateral to the stimulation site. The topography at the N1 latency likewise displayed a lateral distribution for the planar concentric array electrode, however, spreading more towards the central-parietal electrodes. The N2 component displayed clear lateralization for the patch electrode, whereas the planar concentric electrode topography had a more symmetrical and bilateral potential distribution. The topographies of the P2 component were similar for the two electrodes.

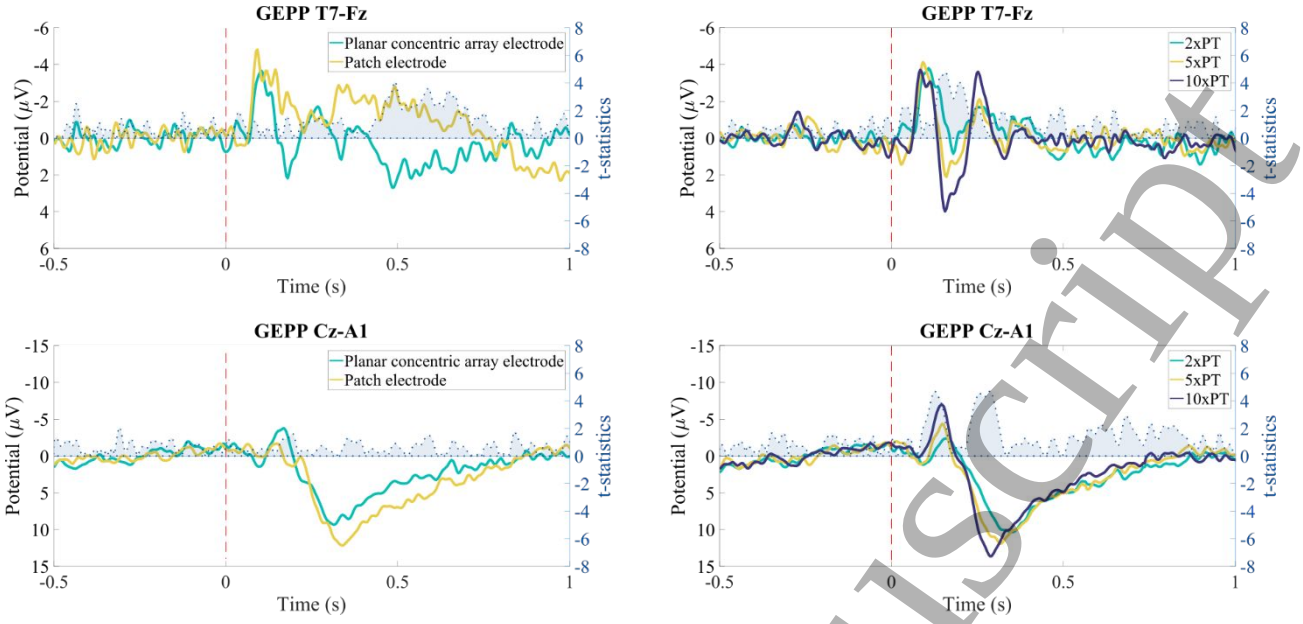

Figure 8: Grand evoked potential predictions (GEPP) and point-by-point t-statistics for electrode (A) and planar concentric array electrode stimulation intensity (B) effects.

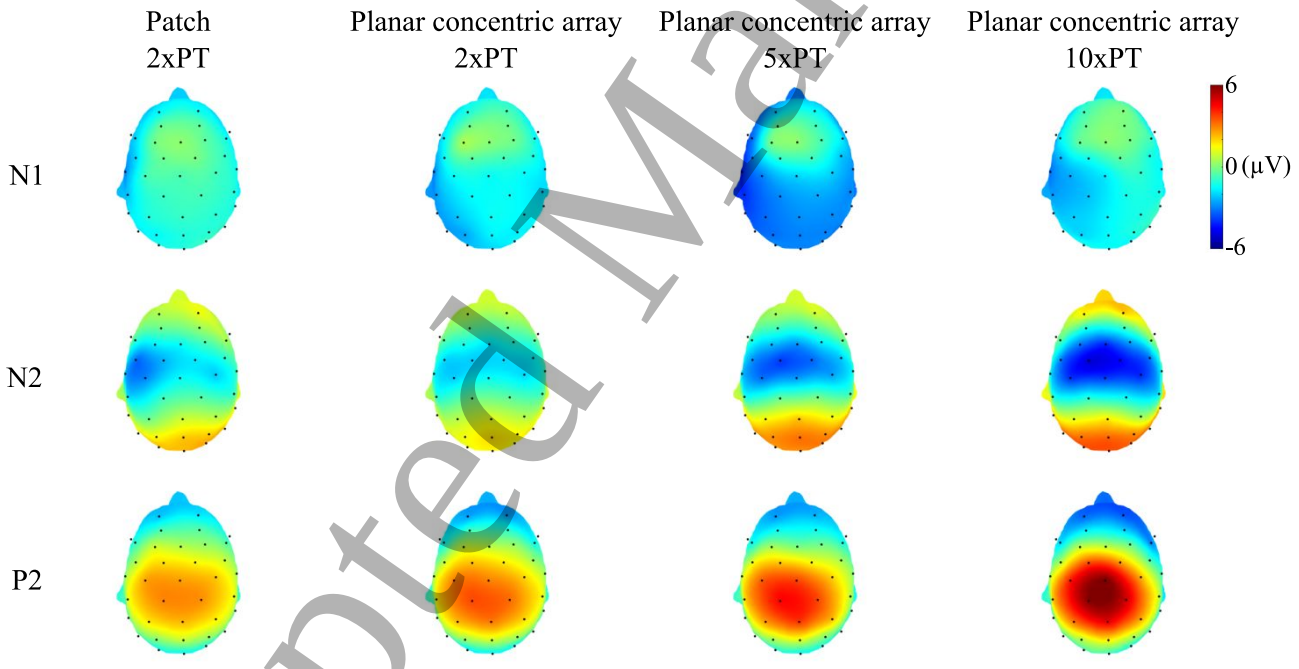

Figure 9: Scalp topography at the GEPP N1, N2, and P2 peak latencies. The first column display topographies for stimulation with the patch electrode, and the last three columns display topographies of stimulation with the planar concentric array electrode at stimulation intensities of 2xPT, 5xPT, and 10xPT, respectively.

4. Discussion

In the present study, significant differences between the planar concentric array electrode and the regular patch electrode were found for PT, psychophysical data, and reaction times. The perception threshold was lower for the planar concentric array electrode, while the stimuli were perceived as more intense (NRS) and sharper. Reaction times were shorter for the patch compared to the planar concentric array electrode. Additionally, the GEPP component latencies of the EPs were longer for the planar concentric array electrode at stimulation intensities of 2xPT. However, this difference was not statistically quantified, and no significant differences were observed for the EP amplitudes. These findings suggest that the presented novel planar concentric array electrode preferentially activates nociceptive fibers for stimulation intensities at PT and 2xPT. Thereby, the population of activated afferents mainly consisted of Aδ-fibers. The NRS ratings and sharpness of the sensation increased with increasing intensity. Furthermore, the reaction times and GEPP peak latencies became shorter as the stimulation intensity increased.

Preferential small fiber activation

PT of the planar concentric array electrode was, in the same range as the PT of the small fiber preferential intra-epidermal electrode (0.21-0.69 mA) and the planar concentric electrode (0.34-0.86 mA)-[11]. The sensation of the stimuli was characterized as sharp for the planar concentric array electrode indicating Aδ-fiber activation. In contrast, the sensation of the patch electrode was dull, which is related to touch sensations mediated by Aβ-fibers [32], [33]. The recorded reaction times were significantly shorter for the patch electrode, which is likely due to the activation of faster-conducting nerve fibers, thus suggesting that the planar concentric array electrode activates a different nerve fiber population compared to the patch. The reaction times for the planar concentric array electrode were 342-408 ms, well within the expected reaction times for Aδ-fiber activation (300-650) [29], [34]. However, the reaction times for the patch electrode were longer (318-379) than expected for Aβ-fiber activation (<300 ms). It is important to notice that reaction times are influenced by the stimulus intensity as well as higher-order processes and are thus not exclusively related to conduction velocity [35]–[37]. Several breaks were included in the experiment, and the order of the electrodes was randomized to minimize attentional differences throughout the experiment. However, cognitive factors such as attention and decision processing may still have affected the observed reaction times [36], [37].

The planar concentric array electrode displayed, on average, 12 ms longer GEPP component latencies compared to the patch. However, this latency shift was not quantified statistically. The scalp map at the latency of the N2 component showed a clear contralateral distribution for the patch electrode, whereas the distribution for the planar concentric array electrode displayed a bilateral pattern. This is in line with previous observations, where non-nociceptive stimulation with patch electrodes displayed lateral components that were not observed for nociceptive stimulation with either intra-epidermal [38] or pin electrodes [39]. The N1 peak distribution were also similar to previous studies [29], [30], however at a current stimulation intensity of 5 time perception threshold, the map is slightly different, probably due to noise alteration.

Preferential small fiber activation at high intensities

The planar concentric electrode design introduced by Kaube *et al.* (2000) has been shown to elicit pinprick sensations [7], [16], [18]; however, at increased stimulation intensities, the sensation changed to an electric shock-like sensation, suggesting Aβ-fiber co-activation [18]. In the present study, the NRS scores increased with increasing intensity. Likewise, the perceived sharpness of the stimulation increased, indicating that the higher intensities were still small fiber preferential and recruited a larger population of nociceptive Aδ-fibers compared to Aβ-fibers. The reaction times at PT and 2xPT were within the normal range observed for Aδ-fibers [29], [35], [40], whereas the 95 % confidence interval of the reaction times for 5xPT and 10xPT included fast reaction times normally considered to be in the range of Aβ-fibers. This may indicate that the planar concentric array electrode is only small fiber preferential at low stimulation intensities, which is comparable to the findings of the intra-epidermal electrode design [3]. Similarly, the latency of the GEPP components at higher intensities corresponds to the latencies observed for the patch electrode or even shorter, which may suggest large fiber activation. On the contrary, no lateralization of the N2-P2 complex was observed in the scalp maps of the planar concentric array electrode, which is yet common for large fiber activation [39]. These findings have multiple possible explanations. A mixed population of activated fibers consisting mainly of small fibers and few large fibers might lead to a dominating sharp sensation potentially masking the sensation quality of activated large fibers, while large fiber responses remain visible in the EP. However, increased nociception due to high-intensity stimuli could also explain the findings as this would increase stimulus saliency and thereby facilitate and speed up the detection of and reaction to the stimulation. Mouraux *et al.* (2013) found that the N1, N2, and P2 components of the nociceptive EP have a clear relation to the saliency of the stimulus and are completely abolished when a relatively short and constant inter-stimulus interval is used. The information of stimulation saliency is likely transmitted through a direct thalamocortical connection providing a fast track of information processing in the presence of highly salient events [41]. Finally, the activation of fast conducting high-threshold mechanoreceptors may pose a possible explanation of the present findings. These fibers display conduction velocities comparable to non-nociceptive mechanosensitive fibers while mediating a sharp pain sensation [42]. The recruitment of such fast conducting nociceptive fibers may increase for high stimulation intensities and thereby contribute significantly to both the stimulus quality and the EP response.

Habituation of small and large fibers

There was a clear increase in the initial estimated PT to the final one after the EEG recording blocks, which indicates habituation. This was more pronounced for the planar concentric array electrode than for the patch electrode. These findings align with those of Hugosdottir *et al.* (2019), which may imply that small fibers habituate more quickly than large fibers to repeated stimulation. On the contrary, Mancini *et al.* (2017) found no difference in the short-term habituation pattern of nociceptive and non-nociceptive EPs across 60 trials. Pronounced small fiber habituation could potentially cause issues when stimulating with small area electrodes, as the stimulation intensity to reach perception might become so high that it leads to co-activation of large fibers. This was not the case in the present study, as the data for high stimulation intensities still suggested small fiber activation. Nevertheless, it is important to consider this aspect when setting up experiments using small fiber preferential

electrodes and adjust the study design accordingly. For example, previous studies showed that threshold habituation could be decreased by the use of double-pulse instead of a single pulse [30]. It is likewise important to notice that in the present study, 60 extra stimulations were applied with the planar concentric array electrode compared to the patch. The perception threshold for the planar concentric array electrode increased by 76% (0.8 % per stimuli) while the perception threshold for the patch electrode increased by only 9% (0.3 % per stimuli, see figure 4). If we assume that the habituation is linearly dependent on the number of stimuli, then 3 times as many stimuli cannot on its own explain the much higher increase in PT for the novel electrode. Furthermore, these extra stimulations were of high intensity, which has been shown to induce less habituation [45], the more pronounced habituation observed for the planar concentric array electrode could merely be a result of the study design rather than the characteristics of the nerve fiber population.

The novel electrode design

Previous modelling studies have shown that smaller cathodes increase the current density within the epidermal skin layer, while the anode size and anode-cathode distance decrease the current spread to deeper tissues and thereby decrease the probability of activating large fibers[11], [20]. The overall result for minimizing the electrode dimensions would thus be increased preferential activation of small fibers. Consequently, the novel electrode in the present study was designed to be as small as possible for a strictly planar and printed electrode. The choice of a planar and printed electrode was made to avoid any protruding elements that could potentially disturb sensations. The novel planar concentric array electrode further has the advantage of being single-use. Additionally, it is small and flexible, making it possible to position the electrode at almost any site on the body. The electrode has several cathode-anode pairs, which increases the probability of placing the electrode close to a nerve fiber as well as the effective area of stimulation. Thereby it is not necessary to reposition the electrode to obtain reasonable thresholds, as is the case with the single cathode intra-epidermal design [29].

The intra-epidermal electrode has previously been found to be the best available electrode for small fiber activation [11], however, high-intensity stimulation is not possible without co-activation of large fibers [3]. The advantage of being able to use higher stimulation intensities is that the electrode may be used to assess small fiber function even in severe neuropathy cases, where the epidermal nerve fiber density is considerably decreased [46], [47]. In addition, an electrode with the possibility to preferentially activate small fibers at high stimulation intensities could be a valuable tool in studies of long-term potentiation where high-frequency high-intensity stimulation is used. The computational model of Poulsen *et al.* (2021) [20] predicted the dimension of the novel planar concentric array electrode to increase preferential small fiber activation compared to the original planar concentric electrode design. Due to the smaller anode-cathode distance and the smaller anode area the activation threshold of the large fibers are expected to increase and thereby increase the activation threshold ratio between large and small fiber and as a result increase the intensity span for which preferential activation of small fibers may be achieved. The psychophysical data in the present study indeed suggests that the novel planar concentric array electrode may achieve preferential small fiber activation, even at high intensities, and is thereby an improvement compared to the original planar concentric design for which sensations changed to indicate large fiber activation when applying high intensity stimuli [18]. The EEG data and reaction time, however, suggests that the novel planar array

electrode design may suffer from similar issues as the intra-epidermal electrode and micropatterned electrode design for high intensity stimulation (approximately above two times perception threshold) is not recommended if preferential small fiber activation is desired [3], [48]. Based on these evidence the novel electrode would be expected to achieve preferential small fiber activation similar to the intra-epidermal and micropatterned electrode design, however, direct comparisons are needed to verify these results and to further explore the possible benefits of the novel electrode design compared to other electrode designs.

5. Conclusion

A novel planar concentric array electrode design was presented and shown to preferentially activate small nociceptive nerve fibers at current stimulations of low intensity. For high intensity stimuli, however the results were contradicting, as reaction times and evoked potentials were within the range expected for large fiber activation, while the psychophysical data revealed intense and sharp sensations. For high current stimulation the targeted nerve fiber population thus likely consists of both large and small fibers, and the contribution of each fiber type is difficult to determine. Further experimental studies involving blocking or denervation of nerve fibers in addition to comparison with other available small fiber preferential electrodes are needed to confirm the electrode performance and to evaluate the range of feasible stimulation intensities. Nevertheless, the small, single-use design may be a valuable tool to investigate small fiber neuropathy and pain mechanisms.

Acknowledgments

The authors have no conflict of interest to declare. The presented work has been funded by the Center for Neuroplasticity and Pain (CNAP), supported by the Danish National Research Foundation (DNRF121).

References

[1] Mouraux, A., Bannister, K., Becker, S., Finn, D. P., Pickering, G., Pogatzki-Zahn, E., and Graven-Nielsen, T., 2021, Challenges and opportunities in translational pain research – An opinion paper of the working group on translational pain research of the European pain federation (EFIC), *Eur. J. Pain (United Kingdom)*, **25**, 731–756.

[2] Plaghki, L. and Mouraux, A., 2003, How do we selectively activate skin nociceptors with a high power infrared laser? Physiology and biophysics of laser stimulation, *Neurophysiol. Clin.*, **33**, 269–277.

[3] Mouraux, A., Iannetti, G. D., and Plaghki, L., 2010, Low intensity intra-epidermal electrical stimulation can activate Aδ-nociceptors selectively, *Pain*, **150**, 199–207.

[4] Inui, K. and Kakigi, R., 2012, Pain perception in humans: use of intraepidermal electrical stimulation, *J. Neurol. Neurosurg. Psychiatry*, **83**, 551–556.

[5] Baumgärtner, U., Greffrath, W., and Treede, R. D., 2012, Contact heat and cold, mechanical, electrical and chemical stimuli to elicit small fiber-evoked potentials: Merits and limitations for basic science and clinical use, *Neurophysiol. Clin.*, **42**, 267–280.

[6] Inui, K., Tran, T. D., Hoshiyama, M., and Kakigi, R., 2002, Preferential stimulation of Aδ fibers by intra-epidermal needle electrode in humans, *Pain*, **96**, 247–252.

[7] Kaube, H., Katsarava, Z., Käufer, T., Diener, H.-C., and Ellrich, J., 2000, A new method to increase nociception specificity of the human blink reflex, *Clin. Neurophysiol.*, **111**, 413–416.

[8] Klein, T., Margerl, W., Hopf, H.-C., Sandkühler, J., and Treede, R.-D., 2004, Perceptual Correlates of Nociceptive Long-Term Potentiation and Long-Term Depression in Humans, *J. Neurosci.*, **24**, 964–971.

[9] Leandri, M., Marinelli, L., Siri, A., and Pellegrino, L., 2018, Micropatterned surface electrode for massive selective stimulation of intraepidermal nociceptive fibres, *J. Neurosci. Methods*, **293**, 17–26.

[10] Mørch, C. D., Hennings, K., and Andersen, O. K., 2011, Estimating nerve excitation thresholds to cutaneous electrical stimulation by finite element modeling combined with a stochastic branching nerve fiber model, *Med. Biol. Eng. Comput.*, **49**, 385–395.

[11] Poulsen, A. H., Tigerholm, J., Meijs, S., Andersen, O. K., and Mørch, C. D., 2020, Comparison of existing electrode designs for preferential activation of cutaneous nociceptors, *J. Neural Eng.*, **17**.

[12] Omori, S., Isose, S., Misawa, S., Watanabe, K., Sekiguchi, Y., Shibuya, K., Beppu, M., Amino, H., and Kuwabara, S., 2017, Pain-related evoked potentials after intraepidermal electrical stimulation to Aδ and C fibers in patients with neuropathic pain, *Neurosci. Res.*, **121**, 43–48.

[13] Kukidome, D. *et al.*, 2016, Measurement of small fibre pain threshold values for the early detection of diabetic polyneuropathy, *Diabet. Med.*, **33**, 62–69.

[14] Katsarava, Z., Yaldizli, Ö., Voulkoudis, C., Diener, H.-C., Kaube, H., and Maschke, M., 2006, Pain related potentials by electrical stimulation of skin for detection of small-fiber neuropathy in HIV, *J. Neurol.*, **253**, 1581–1584.

[15] Lefaucheur, J. P., Ahdab, R., Ayache, S. S., Lefaucheur-Ménard, I., Rouie, D., Tebbal, D., Neves, D. O., and Ciampi de Andrade, D., 2012, Pain-related evoked potentials: A comparative study between electrical stimulation using a concentric planar electrode and laser stimulation using a CO 2 laser, *Neurophysiol. Clin.*, **42**, 199–206.

[16] Katsarava, Z., Ayzenberg, I., Sack, F., Limmroth, V., Diener, H. C., and Kaube, H., 2006, A novel method of eliciting pain-related potentials by transcutaneous electrical stimulation,

Headache, **46**, 1511–1517.
[17] Perchet, C., Frot, M., Charmarty, A., Flores, C., Mazza, S., Magnin, M., and Garcia-Larrea, L., 2012, Do we activate specifically somatosensory thin fibres with the concentric planar electrode? A scalp and intracranial EEG study, *Pain*, **153**, 1244–1252.
[18] La Cesa, S. *et al.*, 2018, Skin denervation does not alter cortical potentials to surface concentric electrode stimulation: A comparison with laser evoked potentials and contact heat evoked potentials, *Eur. J. Pain*, **22**, 161–169.
[19] Legrain, V. and Mouraux, A., 2013, Activating selectively and reliably nociceptive afferents with concentric electrode stimulation: Yes we can! Provided that low stimulus intensities are used!, *Clin. Neurophysiol.*, **124**, 424.
[20] Poulsen, A. H., Tigerholm, J., Andersen, O. K., and Mørch, C. D., 2021, Increased preferential activation of small cutaneous nerve fibers by optimization of electrode design parameters, *J. Neural Eng.*, **18**, 016020.
[21] Hennings, K., Frahm, K. S., Petrini, L., Andersen, O. K., Arendt-Nielsen, L., and Mørch, C. D., 2017, Membrane properties in small cutaneous nerve fibers in humans, *Muscle Nerve*, **55**, 195–201.
[22] Delorme, A. and Makeig, S., 2004, EEGLAB: An open source toolbox for analysis of single-trial EEG dynamics including independent component analysis, *J. Neurosci. Methods*, **134**, 9–21.
[23] Journal, S., Statistical, R., Series, S., and Statistics, C. A., 2010, Symbolic Description of Factorial Models for Analysis of Variance Author (s): G . N . Wilkinson and C . E . Rogers Published by : Blackwell Publishing for the Royal Statistical Society Stable URL : http://www.jstor.org/stable/2346786, **22**, 392–399.
[24] Berg, B. Van Den and Buitenweg, J. R., 2018, Analysis of Nociceptive Evoked Potentials during Multi-Stimulus Experiments using Linear Mixed Models, *40th Annu. Int. Conf. IEEE Eng. Med. Biol. Soc.*, 3048–3051.
[25] van den Berg, B., Doll, R. J., Mentink, A. L. H., Siebenga, P. S., Groeneveld, G. J., and Buitenweg, J. R., 2020, Simultaneous tracking of psychophysical detection thresholds and evoked potentials to study nociceptive processing, *Behav. Res. Methods*, **52**, 1617–1628.
[26] Pernet, C. R., Sajda, P., and Rousselet, G. A., 2011, Single-trial analyses: Why bother?, *Front. Psychol.*, **2**, 1–2.
[27] Barr, D. J., Levy, R., Scheepers, C., and Tily, H. J., 2013, Random effects structure for confirmatory hypothesis testing: Keep it maximal, *J. Mem. Lang.*, **68**, 255–278.
[28] Cruccu, G., Aminoff, M. J., Curio, G., Guerit, J. M., Kakigi, R., Mauguiere, F., Rossini, P. M., Treede, R. D., and Garcia-Larrea, L., 2008, Recommendations for the clinical use of somatosensory-evoked potentials, *Clin. Neurophysiol.*, **119**, 1705–1719.
[29] Mouraux, A., Marot, E., and Legrain, V., 2014, Short trains of intra-epidermal electrical stimulation to elicit reliable behavioral and electrophysiological responses to the selective activation of nociceptors in humans, *Neurosci. Lett.*, **561**, 69–73.
[30] van den Berg, B. and Buitenweg, J. R., 2021, Observation of Nociceptive Processing: Effect of Intra-Epidermal Electric Stimulus Properties on Detection Probability and Evoked Potentials, *Brain Topogr.*, **34**, 139–153.
[31] Mouraux, A., Iannetti, G., and Plaghki, L., 2010, Selective Activation of Aδ Nociceptors By Low-Intensity Intra-Epidermal Electrical Stimulation, *Eur. J. Pain Suppl.*, **4**, 68–68.
[32] Bromm, B. and Meier, W., 1984, The Intracutaneous Stimulus: A New Pain Model for Algesimetric Studies, *Methods Find. Exp. Clin. Pharmacol.*, **6**, 405–410.
[33] Steenbergen, P., Buitenweg, J. R., Trojan, J., van der Heide, E. M., van den Heuvel, T., Flor, H., and Veltink, P. H., 2012, A system for inducing concurrent tactile and nociceptive

sensations at the same site using electrocutaneous stimulation., *Behav. Res. Methods*, **44**, 924–33.

[34] Félix, E. P. V, Giuliano, L. M. P., Tierra-Criollo, C. J., Gronich, G., Braga, N. I. O., Peres, C. A., Nóbrega, J. A. M., and Manzano, G. M., 2009, Sensations and reaction times evoked by electrical sinusoidal stimulation, *Neurophysiol. Clin.*, **39**, 283–290.

[35] Campbell, J. N. and Lamotte, R. H., 1983, Latency to Detection of First Pain, **266**, 203–208.

[36] Kida, T., Nishihira, Æ. Y., and Hatta, Æ. A., 2003, Changes in the somatosensory N250 and P300 by the variation of reaction time, 326–330.

[37] Lele, P. P., Sinclair, D. C., and Weddell, G., 1954, The reaction time to touch, *J. Physiol.*, **123**, 187–203.

[38] Mouraux, A., De Paepe, A. L., Marot, E., Plaghki, L., Iannetti, G. D., and Legrain, V., 2013, Unmasking the obligatory components of nociceptive event-related brain potentials, *J. Neurophysiol.*, **110**, 2312–2324.

[39] Lelic, D., Mørch, C. D., Hennings, K., Andersen, O. K., and Drewes, A. M., 2012, Differences in perception and brain activation following stimulation by large versus small area cutaneous surface electrodes, *Eur. J. Pain*, **16**, 827–837.

[40] Manresa, J. B., Andersen, O. K., Mouraux, A., and van den Broeke, E. N., 2018, High frequency electrical stimulation induces a long-lasting enhancement of event-related potentials but does not change the perception elicited by intra-epidermal electrical stimuli delivered to the area of increased mechanical pinprick sensitivity, *PLoS One*, **13**, 1–19.

[41] Liang, M., Mouraux, A., and Iannetti, G. D., 2013, Bypassing primary sensory cortices-a direct thalamocortical pathway for transmitting salient sensory information, *Cereb. Cortex*, **23**, 1–11.

[42] Nagi, S. S. *et al.*, 2019, An ultrafast system for signaling mechanical pain in human skin, *Sci. Adv.*, **5**, 1–11.

[43] Hugosdottir, R., Mørch, C. D., Andersen, O. K., and Arendt-Nielsen, L., 2019, Investigating stimulation parameters for preferential small-fiber activation using exponentially rising electrical currents, *J. Neurophysiol.*, **122**, 1745–1752.

[44] Mancini, F., Pepe, A., Bernacchia, A., Di Stefano, G., Mouraux, A., and Iannetti, G. D., 2017, Characterising the short-term habituation of event-related evoked potentials, *bioRxiv*, **5**, 1–14.

[45] Von Dincklage, F., Olbrich, H., Baars, J. H., and Rehberg, B., 2013, Habituation of the nociceptive flexion reflex is dependent on inter-stimulus interval and stimulus intensity, *J. Clin. Neurosci.*, **20**, 848–850.

[46] Pittenger, G. L., Ray, M., Burcus, N. I., McNulty, P., Basta, B., and Vinik, A. I., 2004, Intraepidermal Nerve Fibers Are Indicators of Small-Fiber Neuropathy in Both Diabetic and Nondiabetic Patients, *Diabetes Care*, **27**, 1974–1979.

[47] Karlsson, P., Hincker, A. M., Jensen, T. S., Freeman, R., and Haroutounian, S., 2019, Structural, functional, and symptom relations in painful distal symmetric polyneuropathies: a systematic review, *Pain*, **160**, 286–297.

[48] Di Stefano, G. *et al.*, 2020, The new micropatterned interdigitated electrode for selective assessment of the nociceptive system, *Eur. J. Pain (United Kingdom)*, **24**, 956–966.